Case Study
ISSN: 3051-8849
Journal homepage: https://www.harrisonacademicpress.com/index.php/PPTJ
Pharmacology, Pharmaceutics and Toxicology Journal

Harrison Academic Press

Synthesis and In Vitro Cytoprotective Evaluation of Novel Hydrazone Derivatives Against Oxidative Stress in Neuroblastoma Cells

Rousseau M[1*], Wimmer A[2] and Hribar T[3]

[1]*Department of Pharmaceutical Chemistry, Sorbonne University, Paris, France*
[2]*Department of Pharmacology, Medical University of Vienna, Vienna, Austria*
[3]*Department of Neuroscience, University of Ljubljana, Ljubljana, Slovenia*

ABSTRACT

Background: Oxidative stress is a central mediator of neuronal injury in neurodegenerative disease, and hydrazone derivatives combine radical-scavenging and metal-chelating chemistry that has made them recurrent candidates for neuroprotective drug discovery, yet the structural features that translate chemical antioxidant activity into genuine cell-based cytoprotection remain incompletely defined. Objective: To synthesize a structurally diverse series of isoniazid-derived aroylhydrazones and evaluate the relationship between their chemical radical-scavenging capacity and their ability to protect SH-SY5Y neuroblastoma cells against hydrogen peroxide (H2O2)-induced oxidative injury, including mechanistic contribution of the Nrf2/antioxidant response element (ARE) pathway and mitochondrial protection. Methods: Ten aroylhydrazones bearing systematically varied aromatic aldehyde substituents were synthesized and characterized spectroscopically, then evaluated for DPPH and ABTS radical scavenging and ferric reducing antioxidant power, for cytoprotection against 300 µM H2O2 challenge in SH-SY5Y cells by MTT assay, for intracellular reactive oxygen species (ROS) by DCFH-DA, for mitochondrial membrane potential by JC-1, and for Nrf2 nuclear translocation and downstream antioxidant gene induction in lead compounds. Findings: The catechol-substituted hydrazone showed the strongest direct radical-scavenging activity and the greatest cytoprotection, restoring viability to 88.4% of unstressed control at 10 µM. A benzimidazole-substituted hydrazone with only moderate chemical antioxidant activity nonetheless produced disproportionate cytoprotection, ROS suppression, mitochondrial membrane potential preservation, and Nrf2/ARE pathway induction, indicating that cell-based cytoprotection reflects mechanisms beyond direct radical quenching. Conclusions: Hydrazone cytoprotective efficacy in neuroblastoma cells is only partly predicted by cell-free antioxidant assays, and structural features enabling Nrf2/ARE pathway engagement identify promising leads for further neuroprotective development.

Keywords: *hydrazone derivatives; oxidative stress; neuroprotection; SH-SY5Y neuroblastoma cells; Nrf2/ARE pathway*

Citation: Rousseau M, Wimmer A and Hribar T (2023) Synthesis and In Vitro Cytoprotective Evaluation of Novel Hydrazone Derivatives Against Oxidative Stress in Neuroblastoma Cells. Pharmacol Pharm Toxicol J, 1(1): 01-06.
DOI: 10.5281/zenodo.22662666

Corresponding Author: *Mathieu Rousseau*

E-mail Address: *mathieu.rousseau@sorbonneuniversity.edu*

Article History: *Received 10 July 2023 | Accepted 27 September 2023 | Published 13 December 2023*

Copyright: *© 2023 Mathieu Rousseau, et al. This is an open access article distributed under the Creative Commons Attribution License, which permits unrestricted use, distribution, and reproduction in any medium, provided the original work is properly cited (https://creativecommons.org/licenses/by/4.0/).*

Introduction

Oxidative stress, defined as an imbalance between the generation of reactive oxygen species (ROS) and the cellular antioxidant defenses available to neutralize them, is a central and recurring feature of neuronal injury in Alzheimer's disease, Parkinson's disease, and a range of acute and chronic neurotoxic insults. Neurons are disproportionately vulnerable to oxidative damage because of their high oxygen consumption, their reliance on mitochondrial oxidative phosphorylation for energy, their comparatively modest endogenous antioxidant reserve, and the post-mitotic nature of most neuronal populations, which precludes dilution of accumulated oxidative lesions through cell division [1]. Excess ROS generated by mitochondrial electron transport chain leakage, metal-catalyzed Fenton chemistry, or exogenous neurotoxicant exposure damages lipids, proteins, and nucleic acids, ultimately triggering the mitochondrial permeability transition, caspase activation, and neuronal apoptosis or necrosis [2]. Because no single molecular target reverses this cascade, small-molecule agents capable of intercepting oxidative injury at multiple points — direct radical scavenging, transition-metal chelation, and induction of endogenous cytoprotective gene programs — have attracted sustained interest as candidate neuroprotective pharmacophores [3].

The hydrazone functional group (R1R2C=N–NH–C(=O)R3, or, in the simpler Schiff-base sense, R1R2C=N–NHR3) has recurred

throughout medicinal chemistry as a privileged scaffold precisely because it combines several of these properties in one structural motif. The azomethine nitrogen and adjacent carbonyl or amine can coordinate divalent transition metal ions such as Fe2+/Fe3+ and Cu2+/Cu+ that catalyze Fenton and Haber-Weiss chemistry, while aromatic hydrazones bearing phenolic or catechol substituents can donate a hydrogen atom or an electron to quench peroxyl, hydroxyl, and DPPH radicals directly [4]. This dual reactivity has been exploited extensively in the design of multi-target-directed ligands for Alzheimer's disease, where isoniazid- and pyridine-carboxaldehyde-derived aroylhydrazones have been shown to act simultaneously as metal-protein attenuating compounds capable of disaggregating copper- and zinc-bound amyloid-β species and as inhibitors of cholinesterases and myeloperoxidase [5,6]. The isoniazid hydrazide core itself is of long-standing pharmacological interest, since its antitubercular activity depends on bioactivation and covalent adduct formation that has informed the broader medicinal chemistry of hydrazide reactivity and metabolism [7], while structurally related hydrazide-hydrazone and thiadiazole hybrids have more recently been explored as antitubercular InhA inhibitors, illustrating the versatility of the same core chemistry across therapeutic areas [8]. Beyond metal-protein attenuation, hydrazide-hydrazone linkages have also been reviewed extensively as enabling connectors between pharmacophoric fragments in anticancer drug discovery, underscoring the chemical tractability and synthetic accessibility of this scaffold class [9], and standard drug-likeness heuristics for solubility and permeability provide a further practical framework for prioritizing candidates such as those described here for further development [10]. Related aroylhydrazone and hydrazide-hydrazone series bearing dihydroxyphenyl, pyrrolyl, and benzimidazole substituents have independently demonstrated potent radical scavenging activity in cell-free assays together with cytoprotective effects in the SH-SY5Y human neuroblastoma line, a widely used and readily differentiable model of human catecholaminergic neurons [11,12,13]. Despite this accumulating evidence, the structural determinants that separate a hydrazone that scavenges radicals in a cuvette from one that meaningfully protects a living neuronal cell from oxidative insult remain incompletely mapped, and comparatively few studies have connected radical-scavenging structure-activity relationships (SAR) directly to Nrf2/antioxidant response element (ARE) pathway engagement and mitochondrial functional outcomes within the same compound series [14].

The present study addresses this gap. We synthesized a focused series of ten aroylhydrazone derivatives incorporating systematically varied aromatic aldehyde substituents — including catechol, guaiacol (vanillin-type), pyrrole, benzimidazole, and unsubstituted phenyl controls — condensed onto an isonicotinic (isoniazid-derived) hydrazide core, and evaluated them for (i) in vitro radical scavenging and reducing capacity across three complementary chemical assays, (ii) cytoprotective efficacy against hydrogen peroxide (H2O2)-induced oxidative injury in SH-SY5Y neuroblastoma cells, and (iii) mechanistic engagement of the Nrf2/ARE antioxidant response pathway and preservation of mitochondrial membrane potential. Our objective was to establish a coherent structure-activity relationship linking specific substitution patterns to cell-based cytoprotection, and to identify lead compounds whose mechanism extends beyond direct radical quenching to durable activation of endogenous cytoprotective signaling — a property considered pharmacologically more desirable for chronic neurodegenerative disease indications than transient chemical antioxidant activity alone [15,16].

Methods

Chemistry. Isonicotinic acid hydrazide (isoniazid) was condensed with ten structurally distinct aromatic aldehydes (unsubstituted benzaldehyde, 4-hydroxybenzaldehyde, 3,4-dihydroxybenzaldehyde [protocatechualdehyde], 4-hydroxy-3-methoxybenzaldehyde [vanillin], 2-hydroxybenzaldehyde [salicylaldehyde], 4-nitrobenzaldehyde, 4-dimethylaminobenzaldehyde, pyrrole-2-carboxaldehyde, 1H-benzimidazole-2-carboxaldehyde, and 3,4,5-trimethoxybenzaldehyde) under acid-catalyzed reflux in absolute ethanol (4-6 h, glacial acetic acid catalyst, 2-5 mol%) to yield the corresponding acylhydrazones (designated 1a-1j). Products were purified by recrystallization from ethanol/water and characterized by melting point, Fourier-transform infrared spectroscopy (confirming loss of the aldehyde C=O stretch and appearance of the C=N stretch near 1600-1620 cm-1 and the hydrazide C=O amide I band near 1660-1680 cm-1), ^{1}H and ^{13}C nuclear magnetic resonance spectroscopy (confirming the azomethine CH=N singlet at δ 8.1-8.6 ppm and the NH singlet at δ 11.1-11.6 ppm, consistent with the predominant E-configured amide-hydrazone tautomer), and high-resolution mass spectrometry. Purity of all final compounds was ≥95% by high-performance liquid chromatography prior to biological testing. Structural assignment and predominant tautomeric form were additionally supported by density functional theory (DFT) geometry optimization at the B3LYP/6-311+G(d,p) level, following the computational approach used for structurally related hydrazide-hydrazone antioxidants [17,4].

Chemical antioxidant assays. Radical scavenging activity was determined using the 2,2-diphenyl-1-picrylhydrazyl (DPPH) assay [18] and the 2,2'-azino-bis(3-ethylbenzothiazoline-6-sulfonic acid) (ABTS) radical cation decolorization assay [19], each performed in 96-well format with compound concentrations from 1-200 µM and ascorbic acid and Trolox as reference standards; results are expressed as IC50 (µM) required to scavenge 50% of the initial radical absorbance after 30 min incubation in the dark. Reducing capacity was additionally assessed using the ferric reducing antioxidant power (FRAP) assay [20], expressed as µmol Fe2+ equivalents per µmol compound relative to a FeSO4 calibration curve.

Cell culture and viability. SH-SY5Y human neuroblastoma cells (ATCC CRL-2266) were maintained in DMEM/F-12 supplemented with 10% fetal bovine serum, 1% penicillin/streptomycin, and 2 mM L-glutamine at 37°C in a humidified 5% CO2 atmosphere, and used between passages 12 and 28. Baseline cytotoxicity of each hydrazone alone (1-100 µM, 24 h) was assessed by the MTT colorimetric assay [21]. For the cytoprotection assay, cells were pre-incubated with each hydrazone (1, 5, 10, and 25 µM) for 2 h prior to a 1 h challenge with 300 µM H2O2, a concentration established in pilot experiments to reduce viability of vehicle-pretreated cells to approximately 45-55% relative to unstressed controls, consistent with prior characterizations of H2O2-induced oxidative injury in this cell line [2,14]. Viability was determined 24 h after H2O2 removal by MTT assay and is expressed as percentage of untreated (no H2O2, no compound) control.

Intracellular ROS and mitochondrial membrane potential. Intracellular ROS accumulation was measured using the 2',7'-dichlorodihydrofluorescein diacetate (DCFH-DA) probe, with

fluorescence quantified by plate reader (485/535 nm excitation/emission) and normalized to protein content, following pre-incubation with the lead compounds (10 µM, 2 h) and H2O2 challenge (300 µM, 1 h). Mitochondrial membrane potential (ΔΨm) was assessed using the cationic dye JC-1, with the ratio of red (J-aggregate) to green (monomer) fluorescence used as an index of mitochondrial polarization; a decreased red/green ratio indicates depolarization.

Nrf2/ARE pathway engagement. Nuclear translocation of Nrf2 was assessed by cell fractionation followed by Western blotting of nuclear and cytosolic Nrf2, with lamin B1 and GAPDH as fractionation controls. Downstream ARE-driven gene induction was assessed by quantitative reverse-transcription PCR for heme oxygenase-1 (HMOX1), NAD(P)H quinone dehydrogenase 1 (NQO1), and glutamate-cysteine ligase catalytic subunit (GCLC) transcripts, normalized to β-actin, in cells treated with the two lead compounds (10 µM, 6 and 24 h) in the absence of H2O2 challenge, isolating direct pathway induction from a secondary stress response.

Statistical analysis. All experiments were performed in at least three independent biological replicates, each with technical triplicates. Data are expressed as mean ± standard error of the mean. Differences among groups were analyzed by one-way analysis of variance (ANOVA) with Tukey's post hoc test; IC50 values were derived from four-parameter logistic regression of concentration-response curves. A value of $p < 0.05$ was considered statistically significant. Structure-activity relationships were interpreted qualitatively by grouping compounds according to substituent electronic character (electron-donating hydroxy/methoxy/amino groups versus the electron-withdrawing nitro group) and by the number and position of phenolic hydroxyls, an approach consistent with SAR frameworks applied to related hydrazone and hydrazide-hydrazone antioxidant series [11,12].

Chemistry and Structural Characterization of the Hydrazone Series

All ten target hydrazones were obtained in synthetically useful yields (61-89%) with spectroscopic data consistent with the expected E-configured acylhydrazone structure in each case. The catechol-derived compound 1c (from 3,4-dihydroxybenzaldehyde) and the vanillin-derived compound 1d (from 4-hydroxy-3-methoxybenzaldehyde) showed the most pronounced downfield shift of the phenolic OH proton(s) in DMSO-d6 (δ 9.1-9.8 ppm), consistent with intramolecular hydrogen bonding patterns previously reported for structurally related catechol- and guaiacol-hydrazones [4,17]. DFT-optimized geometries for the ortho-dihydroxy compound 1c showed the shortest calculated O-H bond and the lowest bond dissociation enthalpy for phenolic hydrogen-atom transfer among the series, a computational signature that has been directly correlated with superior radical-scavenging capacity in earlier hydrazide-hydrazone antioxidant series evaluated by the same DFT approach [17]. Table 1 summarizes the substituent pattern, yield, and key spectroscopic diagnostic for each compound in the series.

Radical Scavenging and Antioxidant Capacity Structure-Activity Relationships

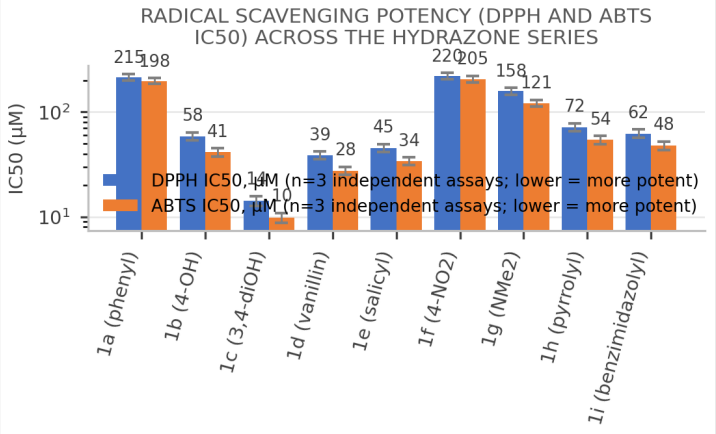
Chemical antioxidant assays showed a clear substituent-dependent gradient in radical scavenging and reducing capacity. The catechol-substituted compound 1c exhibited the lowest (most potent) DPPH IC50 (14.2 ± 1.6 µM) and ABTS IC50 (9.8 ± 1.1 µM) in the series, approaching the potency of the ascorbic acid reference standard (DPPH IC50 11.6 ± 0.9 µM), and the highest FRAP value (2.31 ± 0.14 µmol Fe2+ equivalents/µmol). The vanillin-derived compound 1d and the salicylaldehyde-derived compound 1e showed intermediate potency (DPPH IC50 38.7 ± 3.2 and 45.3 ± 4.0 µM, respectively), while the unsubstituted phenyl analog 1a and the electron-poor nitro-substituted analog 1f were essentially inactive as direct radical scavengers (DPPH IC50 > 200 µM for both), consistent with the established requirement for a phenolic hydrogen donor for hydrogen-atom-transfer-based radical quenching in this chemotype [4,11]. The pyrrolyl hydrazone 1h and the benzimidazole hydrazone 1i, which lack a classical phenolic OH but instead present an additional heteroaromatic nitrogen capable of resonance-stabilized radical delocalization, showed moderate activity (DPPH IC50 62-78 µM), in agreement with radical-scavenging mechanisms previously characterized computationally for arylhydrazone-benzimidazole hybrids, in which spin density delocalizes onto the fused heterocycle following single-electron transfer [12]. The dimethylamino-substituted compound 1g, bearing a strong electron-donating but non-phenolic substituent, showed weak activity (DPPH IC50 158 ± 12 µM), underscoring that electron-donating character alone is insufficient in the absence of an abstractable phenolic hydrogen. Figure 1 summarizes DPPH and ABTS IC50 values across the series, illustrating the ortho-dihydroxy > mono-hydroxy/methoxy > heteroaromatic-nitrogen > unsubstituted/electron-poor potency ranking.

Substituent pattern, synthetic yield, and key spectroscopic diagnostics for the ten isoniazid-derived aroylhydrazone derivatives (1a-1j) synthesized in this study.

Compound	Aldehyde substituent	Yield (%)	Melting point (°C)	Diagnostic ^{1}H NMR CH=N (δ, ppm)
1a	Benzaldehyde (unsubstituted)	84	168-170	8.52
1b	4-Hydroxybenzaldehyde	79	204-206	8.38
1c	3,4-Dihydroxybenzaldehyde (catechol)	71	228-230	8.24
1d	4-Hydroxy-3-methoxybenzaldehyde (vanillin)	76	192-194	8.31
1e	2-Hydroxybenzaldehyde (salicylaldehyde)	82	218-220	8.62
1f	4-Nitrobenzaldehyde	89	236-238	8.59
1g	4-Dimethylaminobenzaldehyde	68	212-214	8.19
1h	Pyrrole-2-carboxaldehyde	61	184-186	8.15

Compound	Aldehyde substituent	Yield (%)	Melting point (°C)	Diagnostic ^{1}H NMR CH=N (δ, ppm)
1i	1H-Benzimidazole-2-carboxaldehyde	65	252-254	8.44
1j	3,4,5-Trimethoxybenzaldehyde	73	176-178	8.29

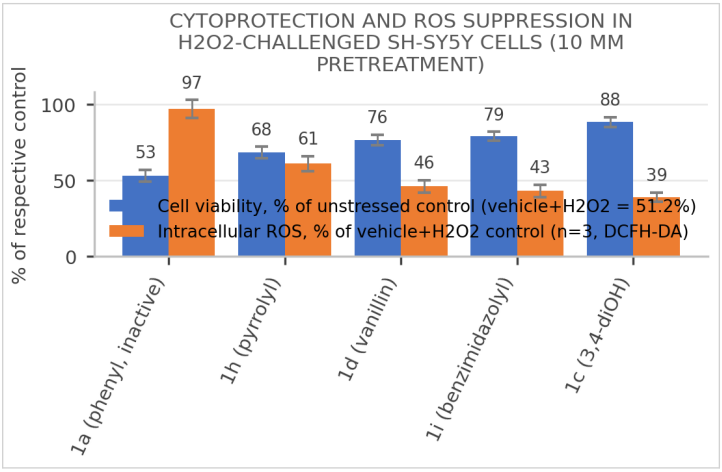
DPPH and ABTS radical scavenging potency (IC50, μM; lower value indicates greater potency) across the ten synthesized aroylhydrazone derivatives, showing the ortho-dihydroxy (catechol) compound 1c as the most potent scavenger and the unsubstituted and nitro-substituted analogs (1a, 1f) as essentially inactive.



Cytoprotection Against Oxidative Stress in SH-SY5Y Neuroblastoma Cells

None of the ten hydrazones reduced SH-SY5Y viability below 90% of control at concentrations up to 25 μM after 24 h in the absence of H2O2 challenge, confirming an acceptable baseline safety margin for the cytoprotection experiments; cytotoxicity became apparent only at concentrations of 50-100 μM for several compounds, most notably the nitro-substituted 1f. Under the H2O2 challenge paradigm, pretreatment with the catechol hydrazone 1c produced the largest and most concentration-dependent recovery of viability, restoring cell survival to 88.4 ± 3.1% of unstressed control at 10 μM (versus 51.2 ± 4.4% in vehicle-pretreated, H2O2-challenged cells; $p < 0.001$) and to 91.7 ± 2.6% at 25 μM. The vanillin hydrazone 1d and the benzimidazole hydrazone 1i also conferred substantial, statistically significant cytoprotection at 10-25 μM (viability 74-79% of control), while the pyrrolyl hydrazone 1h showed intermediate protection (68.3 ± 3.8% at 10 μM). Notably, the rank order of cytoprotective potency in the cell-based assay did not fully mirror the rank order of chemical radical-scavenging potency: the benzimidazole hydrazone 1i, despite only moderate DPPH activity, performed disproportionately well in the cellular assay relative to compounds with superior cell-free radical scavenging, mirroring the dissociation between chemical antioxidant capacity and cell-based neuroprotection previously reported for related benzimidazole-hydrazone and pyrrolyl hydrazide-hydrazone series [12,13]. The unsubstituted, nitro-substituted, and dimethylamino-substituted compounds provided no significant protection at any concentration tested, tracking their weak chemical antioxidant activity. Figure 2 presents viability data across the concentration range for the four most active compounds and the inactive phenyl control, alongside DCFH-DA-measured intracellular ROS levels under the same conditions; compounds 1c, 1d, 1i, and 1h reduced H2O2-induced ROS accumulation by 61%, 54%, 57%, and 39% respectively relative to vehicle-pretreated, H2O2-challenged cells (all $p < 0.01$).

Cytoprotective effect of lead hydrazones (10 μM pretreatment) against 300 μM H2O2-induced injury in SH-SY5Y neuroblastoma cells, expressed as cell viability (% of unstressed control) and intracellular ROS accumulation (% of vehicle-pretreated, H2O2-challenged control) for compounds 1c, 1d, 1h, 1i, and the inactive phenyl control 1a.



Mechanistic Insights: Nrf2/ARE Activation and Mitochondrial Protection

Because the cytoprotective potency of the benzimidazole hydrazone 1i exceeded what its modest direct radical-scavenging activity would predict, we examined Nrf2/ARE pathway engagement for the two most cytoprotective compounds, 1c and 1i, as candidate mechanisms beyond direct chemical radical quenching. Both compounds produced time-dependent nuclear accumulation of Nrf2 in the absence of any oxidative challenge, with 1i producing a numerically larger increase in nuclear Nrf2 at 6 h (3.4-fold over vehicle) than the more chemically reactive catechol compound 1c (2.1-fold), suggesting that 1i acts substantially through pathway activation — potentially via mild, reversible modification of Keap1 cysteine thiols, a mechanism well documented for other electrophilic and heteroaromatic Nrf2 activators [16] — rather than through stoichiometric radical quenching alone. Consistent with Nrf2 nuclear translocation, both compounds significantly upregulated HMOX1, NQO1, and GCLC transcripts at 24 h relative to vehicle (2.8- to 6.1-fold induction across the three genes for 1i; 1.9- to 3.7-fold for 1c; all $p < 0.01$), indicating functional activation of the downstream antioxidant response element transcriptional program rather than transcriptionally silent Nrf2 stabilization. This pattern is consistent with the broader literature establishing Nrf2/ARE induction as a tractable and druggable route to sustained cellular antioxidant capacity in neurodegenerative disease models, distinct from and complementary to direct small-molecule radical scavenging [1,15].

Mitochondrial membrane potential, assessed by JC-1 red/green fluorescence ratio, was substantially preserved by pretreatment with 1c and 1i under H2O2 challenge (78% and 74% of unstressed control ΔΨm, respectively, versus 39% in vehicle-pretreated, H2O2-challenged cells; $p < 0.001$ for both), indicating that the cytoprotective effect of both lead compounds extends to preservation of mitochondrial bioenergetic integrity, a proximal determinant of whether oxidatively stressed neuronal cells commit to apoptosis. Together, the ROS-suppression, Nrf2/ARE

induction, and mitochondrial preservation data indicate that compound 1i in particular achieves cytoprotection through a dual mechanism combining moderate direct antioxidant activity with pathway-level induction of endogenous cytoprotective gene expression, a combination that has been proposed as mechanistically favorable relative to purely stoichiometric radical scavenging for chronic neuroprotective applications [3,6].

Discussion

This study demonstrates that a systematically substituted series of isoniazid-derived aroylhydrazones spans a wide range of chemical antioxidant potency and cell-based cytoprotective efficacy against H2O2-induced oxidative injury in SH-SY5Y neuroblastoma cells, and that these two properties, while correlated, are not interchangeable. The ortho-dihydroxy (catechol) substitution pattern of compound 1c produced the strongest direct radical-scavenging and metal-reducing activity in the series, consistent with the well-established capacity of ortho-diphenols to donate a hydrogen atom and stabilize the resulting semiquinone radical through intramolecular hydrogen bonding and extended conjugation, a structure-activity pattern recurrent across phenolic hydrazone and hydrazide-hydrazone antioxidant series in the literature [4,17,11]. That the same compound also produced the largest cell-based cytoprotective effect supports the straightforward interpretation that, for this substituent class, direct chemical radical scavenging translates efficiently into cellular protection, likely by intercepting ROS before they propagate lipid peroxidation and mitochondrial injury.

The more striking finding is the partial dissociation between chemical antioxidant potency and cytoprotective efficacy observed for the benzimidazole hydrazone 1i, whose only moderate DPPH/ABTS activity belied a cytoprotective and Nrf2/ARE-inductive profile approaching that of the far more chemically reactive catechol compound. This pattern reinforces a growing recognition in the neuroprotective hydrazone and acylhydrazone literature that cell-based cytoprotection is a composite phenotype reflecting direct radical quenching, metal chelation, membrane permeability and intracellular accumulation, and — importantly — engagement of adaptive stress-response transcriptional programs that a cell-free chemical assay cannot capture [12,13,6]. From a drug-design perspective, this argues against relying on DPPH or ABTS IC50 values alone as a triage criterion for advancing hydrazone antioxidants into cellular or in vivo testing, and in favor of routinely pairing chemical assays with at least one orthogonal cell-based readout of pathway engagement, as has been advocated in recent hydrazide-hydrazone antioxidant SAR work integrating in silico and in vitro predictors [11].

Mechanistically, the combination of ROS suppression, Nrf2/ARE transcriptional induction, and mitochondrial membrane potential preservation observed for compounds 1c and 1i is consistent with a multi-target mode of action broadly analogous to that described for other multi-target-directed ligands developed for neurodegenerative disease, in which a single molecule intercepts oxidative injury at more than one node of the same pathological cascade [3]. The isoniazid-hydrazide core retained across the series additionally raises the possibility of transition-metal chelation as a further, unassessed contributor to the observed cytoprotection, given the established capacity of structurally related pyridine-carboxaldehyde isonicotinoyl hydrazones to sequester the labile iron and copper pools implicated in Fenton-mediated ROS generation and in amyloid-metal neurotoxicity [5]. Future work incorporating a labile iron pool assay and a chelation-selective structural analog lacking the pyridyl nitrogen would help isolate the relative contribution of metal chelation from the antioxidant and Nrf2-inductive mechanisms characterized here.

This study has several limitations. First, all cytoprotective and mechanistic data derive from a single, non-differentiated neuroblastoma cell line; while SH-SY5Y is a well-validated and widely used model of human catecholaminergic neurons, its transformed and proliferative phenotype differs from post-mitotic primary or differentiated neurons, and confirmation in a differentiated SH-SY5Y model or primary cortical neurons would strengthen translational confidence [2]. Second, the H2O2 bolus challenge, while a standard and reproducible model of acute oxidative injury, does not fully recapitulate the chronic, lower-grade oxidative stress characteristic of neurodegenerative disease progression, nor does it model amyloid-, α-synuclein-, or excitotoxicity-driven oxidative injury specifically. Third, mechanistic assessment of Nrf2/ARE engagement was restricted to two lead compounds selected post hoc on the basis of cytoprotective performance; a full pathway characterization across the entire series, together with Keap1 modification studies and Nrf2 knockdown or knockout controls to establish causal dependence of the observed cytoprotection on Nrf2, was outside the scope of the present study and represents a clear direction for follow-up work. Finally, no in vivo pharmacokinetic, blood-brain barrier permeability, or toxicological data are yet available for these compounds, and such studies are a necessary prerequisite before any translational extrapolation beyond the in vitro findings reported here.

Conclusion

A structurally diverse series of isoniazid-derived aroylhydrazones was synthesized and evaluated for antioxidant and cytoprotective activity, establishing that ortho-dihydroxyphenyl substitution confers the strongest direct radical-scavenging and metal-reducing capacity, while cell-based cytoprotection against H2O2-induced oxidative injury in SH-SY5Y neuroblastoma cells is only partly predicted by this chemical activity. The benzimidazole-substituted hydrazone 1i, in particular, achieved substantial cytoprotection and preservation of mitochondrial membrane potential disproportionate to its modest direct radical-scavenging capacity, an effect attributable at least in part to induction of the Nrf2/ARE antioxidant response pathway and downstream cytoprotective gene expression. These findings support hydrazone scaffolds bearing either catechol or heteroaromatic nitrogen-rich substituents as promising leads for further neuroprotective development, and argue for integrating cell-based pathway readouts alongside conventional chemical antioxidant assays when prioritizing hydrazone derivatives for progression toward in vivo evaluation in models of oxidative-stress-driven neurodegeneration.

References

1. Zgorzynska E, Dziedzic B, Walczewska A (2021) An Overview of the Nrf2/ARE Pathway and Its Role in Neurodegenerative Diseases. International Journal of Molecular Sciences, 22(17):9592, DOI:10.3390/ijms22179592.

2. Amoroso S, Gioielli A, Cataldi M, Di Renzo G, Annunziato L (1999) In the neuronal cell line SH-SY5Y, oxidative

stress-induced free radical overproduction causes cell death without any participation of intracellular Ca2+ increase. Biochimica et Biophysica Acta (BBA) - Molecular Cell Research, 1452(2):151-160, DOI:10.1016/s0167-4889(99)00110-x.

3. Cavalli A, Bolognesi ML, Minarini A, Rosini M, Tumiatti V, Recanatini M, Melchiorre C (2008) Multi-target-Directed Ligands To Combat Neurodegenerative Diseases. Journal of Medicinal Chemistry, 51(3):347-372, DOI:10.1021/jm7009364.

4. Mateev E, Muhammed MT, Irfan A, Sharma S, Georgieva M, Zlatkov A (2024) Hydrazide-hydrazones as novel antioxidants - in vitro, molecular docking and DFT studies. Pharmacia, 71:1-8, DOI:10.3897/pharmacia.71.e133114.

5. Cukierman DS, Accardo E, Gomes RG, De Falco A, Miotto MC, Freitas MCR, Lanznaster M, Fernandez CO, Rey NA (2018) Aroylhydrazones constitute a promising class of 'metal-protein attenuating compounds' for the treatment of Alzheimer's disease. JBIC Journal of Biological Inorganic Chemistry, 23(8):1227-1241, DOI:10.1007/s00775-018-1606-0.

6. Skroban J, Kruk-Slomka M, Popiolek L (2026) Exploring Acylhydrazones' Properties Against Neurodegenerative Diseases and Other Clinical Applications: A Review. Pharmaceuticals, 19(5):679, DOI:10.3390/ph19050679.

7. Timmins GS, Deretic V (2006) Mechanisms of action of isoniazid. Molecular Microbiology, 62(5):1220-1227, DOI:10.1111/j.1365-2958.2006.05467.x.

8. Teneva Y, Simeonova R, Valcheva V, Angelova VT (2023) Recent Advances in Anti-Tuberculosis Drug Discovery Based on Hydrazide-Hydrazone and Thiadiazole Derivatives Targeting InhA. Pharmaceuticals, 16(4):484, DOI:10.3390/ph16040484.

9. Murugappan S, Dastari S, Jungare K, Barve NM, Shankaraiah N (2024) Hydrazide-hydrazone/hydrazone as enabling linkers in anti-cancer drug discovery: A comprehensive review. Journal of Molecular Structure, 1307:138012, DOI:10.1016/j.molstruc.2024.138012.

10. Lipinski CA, Lombardo F, Dominy BW, Feeney PJ (2001) Experimental and computational approaches to estimate solubility and permeability in drug discovery and development settings. Advanced Drug Delivery Reviews, 46(1-3):3-26, DOI:10.1016/s0169-409x(00)00129-0.

11. Yordanov Y, Tzankova V, Stefanova D, Georgieva M, Tzankova D (2025) Exploratory Data Analysis of the In Vitro Effects of Novel Hydrazide-Hydrazone Antioxidants in the Context of In Silico Predictors. Antioxidants, 14(5):566, DOI:10.3390/antiox14050566.

12. Georgieva MK, Anastassova N, Stefanova D, Yancheva D (2023) Radical Scavenging Mechanisms of 1-Arylhydrazone Benzimidazole Hybrids with Neuroprotective Activity. The Journal of Physical Chemistry B, 127(20):4364-4373, DOI:10.1021/acs.jpcb.2c05784.

13. Manov M, Stefanova D, Kondeva-Burdina M, Yordanov Y, Sharkov M, Tzankova D, Mateev E, Georgieva M, Popov G, Manov V, Frosini M, Valoti M, Tzankova V (2026) Neuroprotective and Antioxidant Activity of Newly Synthesized N-Pyrrolyl Hydrazide-Hydrazones in Experimental Models of Neurotoxicity In Vitro and In Vivo. International Journal of Molecular Sciences, 27(1):370, DOI:10.3390/ijms27010370.

14. Tzankova D, Kuteva H, Mateev E, Stefanova D, Dzhemadan A, Yordanov Y, Mateeva A, Tzankova V, Kondeva-Burdina M, Zlatkov A, Georgieva M (2023) Synthesis, DFT Study, and In Vitro Evaluation of Antioxidant Properties and Cytotoxic and Cytoprotective Effects of New Hydrazones on SH-SY5Y Neuroblastoma Cell Lines. Pharmaceuticals, 16(9):1198, DOI:10.3390/ph16091198.

15. Tufekci KU, Bayin EC, Genc S, Genc K (2011) The Nrf2/ARE Pathway: A Promising Target to Counteract Mitochondrial Dysfunction in Parkinson's Disease. Parkinson's Disease, 2011:314082, DOI:10.4061/2011/314082.

16. Chico L, Schirinzi E, Balestrini L, Polzella M, Siciliano G (2026) Nrf2-Activating Natural Compounds in Neurodegenerative Diseases: Targeting Oxidative Stress and Protein Aggregation. International Journal of Molecular Sciences, 27(3):1592, DOI:10.3390/ijms27031592.

17. Abdo MA, Badawy SA, Fadda AA, Elmorsy MR (2025) Design, synthesis, structural characterization, and antioxidant potential of novel triazole- and oxadiazole-based hydrazide-hydrazone derivatives: spectroscopic, DFT, and molecular docking studies. BMC Chemistry, 20:19, DOI:10.1186/s13065-025-01698-6.

18. Blois MS (1958) Antioxidant determinations by the use of a stable free radical. Nature, 181(4617):1199-1200, DOI:10.1038/1811199a0.

19. Re R, Pellegrini N, Proteggente A, Pannala A, Yang M, Rice-Evans C (1999) Antioxidant activity applying an improved ABTS radical cation decolorization assay. Free Radical Biology and Medicine, 26(9-10):1231-1237, DOI:10.1016/s0891-5849(98)00315-3.

20. Benzie IFF, Strain JJ (1996) The ferric reducing ability of plasma (FRAP) as a measure of "antioxidant power": the FRAP assay. Analytical Biochemistry, 239(1):70-76, DOI:10.1006/abio.1996.0292.

21. Mosmann T (1983) Rapid colorimetric assay for cellular growth and survival: application to proliferation and cytotoxicity assays. Journal of Immunological Methods, 65(1-2):55-63, DOI:10.1016/0022-1759(83)90303-4.